

Design and Validation of an offline Oceanic Tracer Transport model using Re-analysis Ocean Currents

Vinu Valsala¹, Shamil Maksyutov¹ and Motoyoshi Ikeda²

¹CGER, National Institute for Environmental Studies, Tsukuba, Ibaraki, Japan.

²Graduate School of Environmental Science, Hokkaido University, Sapporo, Japan

Correspondence: vinu.valsala@nies.go.jp

1. INTRODUCTION

An offline model for ocean tracer transport is devised and applied to a conservative tracer and results are validated. This model makes use of precalculated 3-dimensional model transport vectors, mixing coefficients and diffusion tensors from an online run which is recorded at a regular interval of time. Here the word “offline” means that we do not model the ocean currents or stratification explicitly. Instead, they are borrowed from some other model outputs (say from a re-analysis product) which we refer to as “online data”. These “online” variables are archived and interpolated into adequate time step in order to evolve the prognostic passive tracer. The advantages of solving passive tracers in this manner are manifold. The numerical stability constraints for momentum equation solving (for example C.F.L limits) can be relaxed in an offline passive tracer simulation because oceanic velocities are an order of magnitude smaller than the wave speed (here, concern is given on internal modes resolved in the numerical solutions for momentum equations) associated with the momentum evolution. Therefore model time steps can be increased and computational time can be saved efficiently. Being advantage from saving computational time, the offline models can thus be more focused on a higher resolution configurations. High resolution is necessary to account for the subgrid scale transport of the passive tracers.

2. DESIGN OF THE MODEL

The evolution of any conservative tracer concentration 'C' can be written as,

$$\partial C/\partial t + U \cdot \nabla_H C + W \partial C/\partial z = \partial/\partial z (K_z \partial/\partial z C) + \nabla_H \cdot (K_h \nabla_H C) + \phi \quad (1)$$

where ∇_H is the horizontal gradient operator, U is the horizontal velocity, W is the vertical velocity, K_z is the vertical mixing coefficient and K_h is the two dimensional diffusion tensor. A term ϕ is added to the R.H.S of the equation (1) in order to represent any sink or source, which can be interpreted as internal consumption or production of the tracer as well as the surface intake and efflux.

2a. Vertical mixing

We have opted for a K-Profile Parameterization (KPP henceforth) for the vertical mixing. In KPP

parameterization the vertical mixing is resolved by generating a non-local k-profile which falls within the mixed layer yielding a depth dependent mixing coefficient (K_x) as,

$$K_x(\sigma) = h w_x(\sigma) G(\sigma) \quad (2)$$

where ($\sigma = d/h$) is the scaling of depth within the mixed layer (h) whose value ranges from zero at the surface to one at the bottom of the mixed layer. $G(\sigma)$ is a cubic polynomial shape function,

$$G(\sigma) = a_0 + a_1\sigma + a_2\sigma^2 + a_3\sigma^3 \quad (3)$$

where, the a_0 , a_1 , a_2 and a_3 are the coefficients which controls the diffusivities and their derivatives at both the top and bottom of the mixed layer. The values for these coefficients are chosen from Large et al. (1994). In a stable condition the turbulent velocity scale w_x in equation (2) has two key forms as,

$$w_x = \kappa(a_x u_*^3 + c_x \kappa \sigma w_*^3)^{1/3} \quad \text{if } \sigma < \varepsilon \quad (4)$$

$$w_x = \kappa(a_x u_*^3 + c_x \kappa \varepsilon w_*^3)^{1/3} \quad \text{if } \varepsilon < \sigma < 1 \quad (5)$$

The ε is the non-dimensional extent of the surface layer which we chosen as $\varepsilon = 0.1$ as in Large et al. (1994). The κ is the von Karman's constant (0.40). The a_x and c_x are the coefficients of non-dimensional flux profiles for the tracers whose values are chosen as $a_x = -28.86$ and $c_x = 98.96$.

2b. Horizontal mixing

K_h and K_z collectively represent the three-dimensional tensor. The diffusion tensor incorporates diffusion fluxes rotated tangential to the local isopycnals, the so-called isopycnal diffusion, a process which is important for ocean ventilation in the high latitude. In our version of offline model, we incorporate both Redi fluxes and GM fluxes in the tracer equation as,

$$\partial C / \partial t + \mathbf{U} \cdot \nabla C + \nabla_z [C \partial / \partial z (K_h \nabla_z \rho / \rho_z)] - \partial / \partial z [C \nabla \cdot (K_h \nabla_z \rho / \rho_z)] = R(C) + (\text{other terms}) \quad (6)$$

Apart from the isopycnal mixing, a weak Laplacian diffusion is provided for computational stability where sharp concentration gradient occurs. The effect of this Laplacian diffusion is set to minimal because such lateral diffusion results in unrealistic mixing and smeared ventilations (Dutay et al., 2002). The coefficient for Laplacian mixing is taken as a function of latitude (θ) as $Ah(\theta) = A_{hback} \cos(\theta)^{1/5}$ in which A_{hback} is set at $2.0 \times 10^2 \text{ m}^2 \text{ s}^{-1}$. This yields a diffusion coefficient tapered to a minimum value of $20 \text{ m}^2 \text{ s}^{-1}$ at polar region in converging meridian.

2c. Grids

The offline model takes the velocity fields and stratification from a precalculated archive. Thus the grid design depends on the parent model from which the offline fields are borrowed. In most of the General Circulation Models, the volume is conserved in every grid cell locally because water is incompressible (Boussinesq approximation is made) and velocities can be interpolated into desired grid and thus the choice of grid becomes non mandatory. However, this assumption is not applicable

in a non-rigid-lid model where surface volume is changing with rainfall and evaporation. In this article we describe the model in B-grid structure, as it is done in the parent online model, in which the velocities are at the corners of the tracer grids. The tracer equation (1) is solved using the flux form where velocities at the cell faces are multiplied by the tracers at the same location and found a gradient of the fluxes.

3. DATA AND MODEL EXPERIMENTS

We use the flow vectors and stratification (i.e. temperature and salinity) derived from ocean assimilation product of GFDL (Geophysical Fluid Dynamics Laboratory). The model configuration of assimilated products contains Modular Ocean Model-4 (MOM4-SIS) ocean/ice component coupled to Climate Model (CM2.1) with assimilation of in-situ temperature profiles from NODC (National Oceanographic Data Center) archives using 3-D variational scheme. The data is obtained from <http://data1.gfdl.noaa.gov/nomads/forms/assimilation.html>. This data set has a resolution of 1° zonally with 360 grid points. Latitudinal resolution is 1° at the poles with a high resolution (0.8°) in the tropics containing a total of 200 grid points. Model contains 50 vertical levels with 10 meter resolution in the upper 225m and stretched vertical intervals below the depth by including 30 levels in the upper 500m. With this high vertical resolution, the entrainment and vertical velocities might be resolved explicitly in the data while vertical mixing has to be parameterized. The mixed layer depth is borrowed from the same assimilation data. The assimilated currents, stratification and mixed layer depth are obtained for 15 years. A monthly average value from the 15 years is constructed.

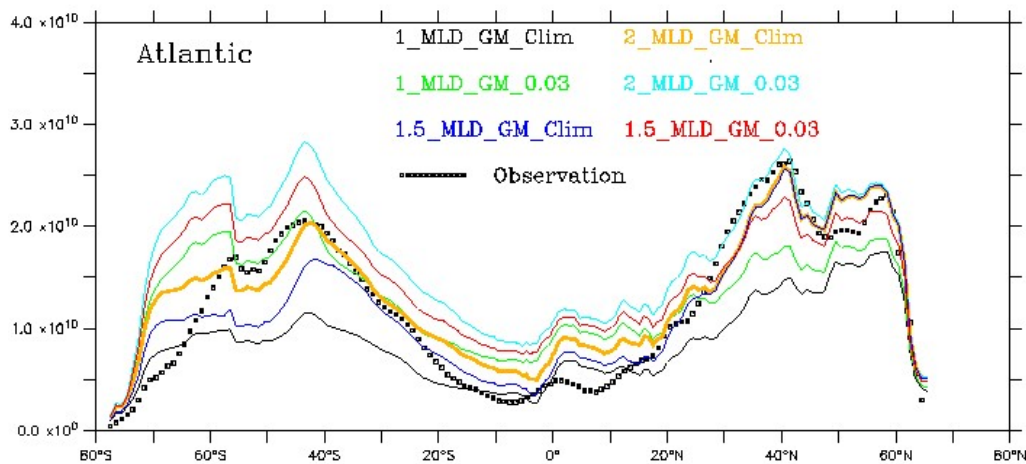


FIGURE 1. CFC-11 concentration integrated zonally and vertically over Atlantic Ocean Units are in picomole $\text{m}^2 \text{kg}^{-1}$.

3a. CFC-11 simulation

The model is forced with surface concentration of CFC-11 in the atmosphere provided by OCMIP-II flux protocol (Dutay et al. (2002)). The surface CFC-11 flux is calculated as $F = K_w (C_{sat} - C_{surf})$ where the K_w is the piston velocity (ms^{-1}) with which the CFC is injected into the ocean depending on the wind variance and sea surface temperature. The C_{sat} (mol m^{-3}) is the saturation level of CFC in the surface of the ocean which depends on the atmospheric pressure, solubility for water-vapor saturated air and partial pressure of CFC in dry air at one atmosphere total pressure. C_{surf} (mol m^{-3}) is the model surface concentration of CFC-11. This is the standard OCMIP-II flux protocol for CFC calculation and we kept the same forcing as that of candidate models participated in OCMIP-II (Dutay et al., 2002).

3b. Comparison with OCMIP-II participant models

Figure 2 shows the zonally-integrated CFC-11 column inventories in the entire Atlantic (100° W to 20° E) as simulated by candidate models of OCMIP-II, our model and the corresponding observations. This provides a quantitative comparison of CFC-11 simulated by each of these models. The northern Atlantic ventilation process is captured by participating models of OCMIP-II although majorities underestimate it. A close examination indicates that our model has an excellent agreement with the observations in the subduction zone of the northern Atlantic. The model spread is relatively larger in the northern Atlantic than in the Southern Ocean. Among the OCMIP-II candidates, a double peak in the north Atlantic is captured only in MIT, IGCR and NERSC although the amplitude is almost double in NERSC. The other candidates do not have an obvious double peak. It is noticeable that our model captures these two maxima remarkably well compared to the observations.

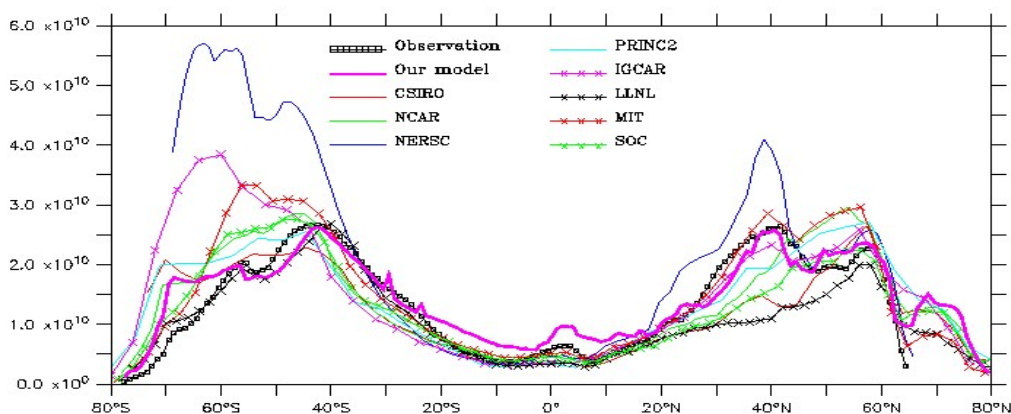


FIGURE 2. Zonally integrated column inventories of CFC-11 in entire Atlantic from candidate models of OCMIP-II, our model and corresponding observation. Units are in picomole $\text{m}^2 \text{kg}^{-1}$.

3c. Error comparison with OCMIP-II participant models

The Taylor (2001) diagram (Figure 3) explicitly shows the correlation coefficient between the observed field and the model as well as their centered root-mean-square (RMS) differences, along with the ratio of the standard deviations of the two patterns. The centered RMS difference between the model and the observations is proportional to their distance apart in the same units as the standard deviation. This distance is 0.14×10^{10} picomole $m^2 kg^{-1}$ in our model. This represents the RMS difference of the model north-south column inventory from the observations. In our model this corresponds to an error of $\pm 8\%$ from the observed mean of north-south CFC-11 column inventory. Among the OCMIP-II participant models, CSIRO and LLNL have the same RMS error difference as ours. The RMS error differences of NCAR and MIT are $\pm 4\%$ and $\pm 9\%$, respectively. This shows that these models (including ours) have error in the amplitude of the north-south column inventory. In our model, this is due to the exaggeration of vertical mixing and CFC-1 uptake in the equatorial region. The overall error in the tropics in our model is 30%. However, observations suggest that the tropical Atlantic contains only 18.7% of the total CFC-11 of the entire Atlantic and thus a model error of 30% in the tropics means only an error of 6% in the total CFC-11 uptake. The minimum RMS error difference of OCMIP-II participants are found in PRINC2 and SO which have an error of $\pm 4\%$ from the mean north-south column inventory.

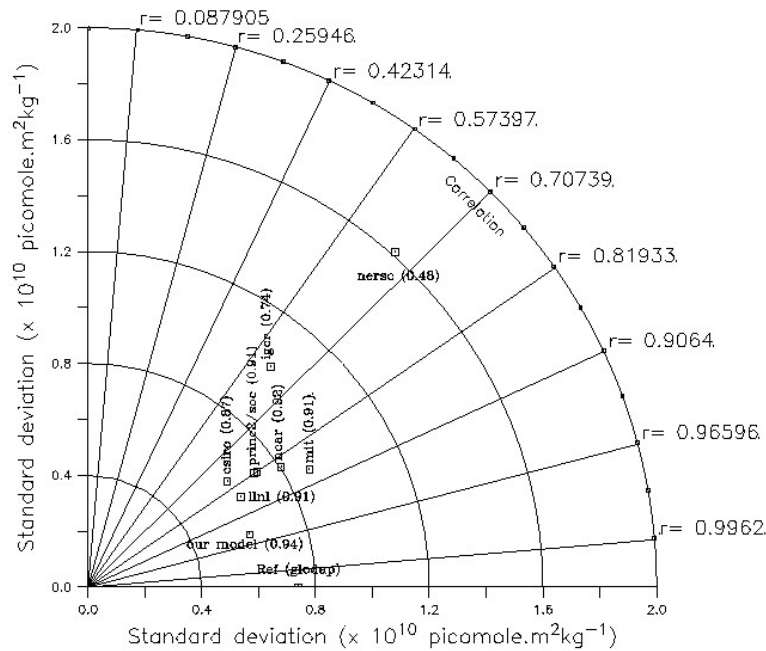


FIGURE 3. Model standard deviation and correlation with reference data (GLODAP) is displayed as in Taylor (2001). The radial lines are labeled by the cosine of the angle made with the abscissa.

The reference data has a standard deviation of 0.74. Our model has a standard deviation of 0.60 and correlation coefficient 0.95. Skill values are given in brackets.

4. SUMMARY

An offline passive tracer transport model is designed and discussed here. This model is developed in NIES under carbon cycle research project inside the GOSAT (Greenhouse gas Observing SATellite) modeling group. The model equations for tracer evolution, vertical mixing, horizontal diffusion and other sub-grid scale parameterizations are detailed. The model borrows offline fields from precalculated monthly archives of assimilated ocean currents, temperature and salinity, and evolves a prognostic passive tracer with prescribed surface forcing. The model's performance is validated by simulating CFC-11 cycle in the ocean starting from the pre-industrial period (1938) with observed anthropogenic perturbations of atmospheric CFC-11 to comply with OCMIP-II flux protocol. The model results are compared with ship observations as well as the results of candidate models of OCMIP-II and a performance is assessed. The model simulates the deep ventilation processes in the Atlantic ocean appreciably well and yields a good agreement in column inventory of CFC-11 compared to the observation. The error estimates show that the models intake of CFC-11 is within an over all error bar of $\pm 8\%$ in the Atlantic, while an exaggeration in tropical CFC-11 intake is noted. The spatial pattern of CFC-11 intake is well simulated in the model with an overall Atlantic correlation of 0.95 compared to the observations. The statistical skill comparison test with the OCMIP-II participant models shows that our model performs appreciably well in the CFC-11 column inventory simulation. The spatial pattern of CFC-11 inventories in our model have higher correlation with the observations than the OCMIP-II participant models. The improvements in performance of our model compared to other models are attributed to its higher resolution and assimilated offline inputs feeding. This shows a potential role in improving transport calculation in the ocean with cost-effective computation.

REFERENCE

Dutay, J. C. and Coauthors, 2002: Evaluation of ocean model ventilation with CFC-11; comparison of 13 global ocean models. *Ocean Modelling*, 4, 89-120.

Large, W. G., J. C. McWilliams, and S. C. Doney, 1994: Ocean vertical mixing: A review and a model with a nonlocal boundary layer parameterization. *Rev. Geophys.*, 32, 363-403.

Valsala K. V., S. Maksyutov and M. Ikeda, 2007: Design and Validation of an offline Oceanic Tracer Transport Model for Carbon Cycle Study, *J. Climate*, (in press).